THE JOURNAL OF BIOLOGICAL CHEMISTRY VOL. 286, NO. 16, pp. 14724–14736, April 22, 2011

An N-terminal Polybasic Domain and Cell Surface Localization Are Required for Mutant Prion Protein Toxicity*[S]

Received for publication, December 21, 2010, and in revised form, March 3, 2011 Published, JBC Papers in Press, March 8, 2011, DOI 10.1074/jbc.M110.214973

Isaac H. Solomon[‡1], Natasha Khatri[‡], Emiliano Biasini[‡], Tania Massignan[‡], James E. Huettner[§], and David A. Harris[‡2]

From the [‡]Department of Biochemistry, Boston University School of Medicine, Boston, Massachusetts 02118 and the [§]Department of Cell Biology and Physiology, Washington University School of Medicine, St. Louis, Missouri 63110

There is evidence that alterations in the normal physiological activity of PrP^C contribute to prion-induced neurotoxicity. This mechanism has been difficult to investigate, however, because the normal function of PrP^C has remained obscure, and there are no assays available to measure it. We recently reported that cells expressing PrP deleted for residues 105–125 exhibit spontaneous ionic currents and hypersensitivity to certain classes of cationic drugs. Here, we utilize cell culture assays based on these two phenomena to test how changes in PrP sequence and/or cellular localization affect the functional activity of the protein. We report that the toxic activity of Δ105–125 PrP requires localization to the plasma membrane and depends on the presence of a polybasic amino acid segment at the N terminus of PrP. Several different deletions spanning the central region as well as three disease-associated point mutations also confer toxic activity on PrP. The sequence domains identified in our study are also critical for PrP^{Sc} formation, suggesting that common structural features may govern both the functional activity of PrP^C and its conversion to PrP^{Sc}.

Prion diseases or transmissible spongiform encephalopathies comprise a group of fatal neurodegenerative disorders in humans and animals that can be sporadic, infectious, or genetic in origin (1, 2). The prion protein (PrP^C) is a membrane-anchored glycoprotein with no widely agreed-upon physiological function, although its ability to convert into a self-propagating isoform (PrP^{Sc}) is associated with development of prion diseases. PrP^C, thus, plays a crucial role in prion pathogenesis as a substrate for generation of PrP^{Sc}, a conclusion that has been demonstrated by the resistance of PrP-null mice to prion infection (3). In addition, however, there is evidence that PrP^C is required for delivery of a toxic signal during prion propagation. This is demonstrated by the fact that brain tissue from PrP-null mice grafted into wild-type animals remains healthy despite the presence of copious amounts of PrP^{Sc} from the surrounding host brain (4). Moreover, conditional genetic ablation of neuronal PrP^C allows pathological and clinical recovery of prion-infected mice (5). Therefore, prion neurotoxicity is likely due to subversion of normal PrP^C function rather than loss of PrP^C or gain of PrP^{Sc} activity (6).

However, progress in investigating this mechanism has been hampered by a lack of understanding of the physiological role of PrP^C and the absence of assays to measure the functional activity of the protein. To address this issue, our laboratory has recently developed two assays that measure toxicity of PrP mutants expressed in cultured cells. The first assay is a drug-based cellular assay (DBCA)[3] that measures cell death resulting from increased accumulation of two classes of drugs that are normally used to select transfected cell lines (aminoglycosides and bleomycin analogues) (7, 8). The second assay utilizes whole-cell patch clamping to measure the large spontaneous cationic currents associated with mutant PrP expression (9). We have hypothesized that these currents are generated by PrP-containing ion channels or pores in the plasma membrane that may facilitate the increased influx of drugs into cells observed in the DBCA. These two assays, which measure functional activities of PrP^C, provide powerful tools for identifying structural domains and cellular compartments that are essential for PrP toxicity, information that could otherwise be obtained only by the creation and characterization of multiple transgenic mouse lines.

In both the DBCA and patch clamp assay, the largest effects are observed for Δ105–125 PrP (referred to as ΔCR PrP), a deletion mutant that is missing 21 highly conserved residues in the central region of the protein. Transgenic mice expressing this molecule develop severe neurological illness that can be rescued by overexpressing wild-type PrP (10). ΔCR PrP is neither aggregated nor protease-resistant and has cellular localization identical to that of WT PrP, suggesting that its toxicity is due to an alteration of the normal function of PrP^C (10, 11). Therefore, we have selected ΔCR PrP as a starting point in our analysis of the structural and cellular determinants of PrP toxicity. Importantly, several of the sequence domains identified in our study as being essential for PrP toxicity have been previously reported to be critical for PrP^{Sc} formation, suggesting that common structural features may govern both the functional activity of PrP^C and its conversion to PrP^{Sc}. Therefore, small

* This work was supported, in whole or in part, by National Institutes of Health Grants NS052526 and NS040975 (to D. A. H.) and NS30888 (to J. E. H.).

[S] The on-line version of this article (available at http://www.jbc.org) contains supplemental Fig. 1.

[1] Supported by National Institutes of Health Pre-doctoral Fellowship NS063547 and the Medical Scientist Training Program at Washington University (National Institutes of Health Grant T32GM007200).

[2] To whom correspondence should be addressed: Dept. of Biochemistry, Boston University School of Medicine, 72 East Concord St., K225, Boston, MA 02118. Tel.: 617-638-4362; Fax: 617-638-5339; E-mail: daharris@bu.edu.

[3] The abbreviations used are: DBCA, drug-based cellular assay; M6PR, mannose 6-phosphate receptor; MTT, 3-(4,5-dimethylthiazol-2-yl)-2,5-diphenyltetrazolium bromide; DRM, detergent-resistant membrane; GAG, glycosaminoglycan; GSS, Gerstmann-Sträussler-Scheinker; CJD, Creutzfeldt-Jakob Disease; GPI, glycosylphosphatidylinositol; ER, endoplasmic reticulum; CR, central region.

molecules capable of blocking mutant PrP toxicity in our cellular assays may be valuable as anti-prion therapeutics.

EXPERIMENTAL PROCEDURES

Cells and Constructs—HEK293 cells (ATCC CRL-1573) were maintained in α-minimum essential medium/Dulbecco's modified Eagle's medium (1:1) supplemented with nonessential amino acids, L-glutamine, 10% fetal bovine serum, penicillin/streptomycin, and 50 μg/ml hygromycin. Stable lines were created by transfecting HEK cells with pcDNA3.1(+)Hygro (Invitrogen) vector alone or with vector containing the cDNA sequence for WT or mutant murine PrP using Lipofectamine 2000 (Invitrogen) according to the manufacturer's directions. Clones were selected for 14 days in 200 μg/ml hygromycin. Except where noted (Figs. 7–9), WT PrP contained an epitope tag (L108M/V111M) for the monoclonal antibody 3F4 (12). Deletions and point mutations were introduced into WT PrP using a QuikChange site-directed mutagenesis kit (Stratagene). The sequences for Δ105–125 (ΔCR) PrP and PG14 have been described previously (10, 13). The chimeric transmembrane PrP construct ΔCR PrP-mannose 6-phosphate receptor (M6PR) was generated by ligating cDNA encoding amino acids 1–230 of mouse PrP to the transmembrane and truncated cytoplasmic domains of a mutant bovine cation-independent M6PR, as described previously (14). The ER retention signal KKMP was introduced at the C terminus of the ΔCR PrP-M6PR construct using a QuikChange site-directed mutagenesis kit. ΔCR PrP-Golgi was constructed by ligating cDNA encoding amino acids 1–230 of mouse PrP to the transmembrane domain of rubella virus envelope glycoprotein E2 (amino acids 238–255) (15).

Western Blotting and Immunofluorescence Staining—Western blots were probed with anti-PrP antibodies 6D11 (16) or 6H4 (17) followed by goat anti-mouse IgG (Pierce) and developed with ECL (GE Healthcare). Some of the samples in Fig. 5*D* were deglycosylated by treatment with either *N*-glycosidase F or endoglycosidase H (New England Biolabs, Beverly, MA) according to the manufacturer's directions. Immunofluorescence staining was performed by fixing cells in 4% paraformaldehyde in PBS, permeabilizing with Triton X-100 in PBS, and labeling with 6D11 and Alexa-488 goat anti-mouse IgG (Molecular Probes). Antibodies against giantin (Covance) and protein disulfide isomerase (Sigma) were used to label the Golgi and ER, respectively, followed by Alexa-594 goat anti-rabbit IgG (Molecular Probes). For surface staining, living cells were incubated on ice with 6D11, after which they were fixed and labeled with Alexa-488 goat anti-mouse IgG. Cells were viewed with 40× or 100× objectives on a Nikon TE-2000E inverted fluorescence microscope, and images were captured with METAMORPH software (Molecular Devices, Sunnyvale, CA).

Electrophysiology—Assay of spontaneous channel activity was performed by whole-cell patch clamping using standard techniques as previously described (9, 18, 19). Pipettes were pulled from borosilicate glass, coated with Sylgard, and polished to an open resistance of 1–10 megaohms. Experiments were conducted at room temperature with the following solutions: internal: 140 mM cesium glucuronate, 5 mM CsCl, 4 mM MgATP, 1 mM Na_2GTP, 10 mM EGTA, and 10 mM HEPES (pH 7.4 with CsOH); external: 150 mM NaCl, 4 mM KCl, 2 mM $CaCl_2$, 2 mM $MgCl_2$, 10 mM glucose, and 10 mM HEPES (pH 7.4 with NaOH). Current signals were collected from an Axopatch 200B amplifier and digitized with a Digidata 1330 interface (Axon Instruments) or with an EPC-10 amplifier controlled by PatchMaster acquisition software (HEKA Elektronik) and were saved to disc for analysis with PClamp 9 software. Current activity was plotted as the proportion of total recording time that a cell exhibited inward current ≥450 pA.

DBCA—Cell death in response to G418 treatment was assayed as previously described (7, 8). Confluent cells in 24-well plates were incubated in medium lacking hygromycin with either 0 or 400 μg/ml G418 for 24 h at 37 °C. The medium was removed, and cells were incubated with 3-(4,5-dimethylthiazol-2-yl)-2,5-diphenyltetrazolium bromide (MTT) (1 mg/ml in PBS) for 30 min at 37 °C. The MTT was then removed, cells were solubilized in 200 μl of DMSO, and A_{570} was measured in a plate reader (Bio-Rad). Cell death was calculated by subtracting the percentage of treated to untreated A_{570} values from 100%.

Isolation of Detergent-resistant Membrane Domains—Detergent-resistant membrane (DRM) domains were isolated as previously described (20). Cells were resuspended in cold buffer (25 mM Tris-HCl, pH 7.4, 150 mM NaCl, 5 mM EDTA, and 1% Triton X-100) and incubated for 30 min on ice. Lysates were mixed with 60% Opti-Prep (Sigma) to reach a final concentration of 40% Opti-Prep. A step gradient was created by overlaying the lysates with 30 and 0% Opti-Prep. Samples were ultracentrifuged at 172,000 × *g* for 4 h at 4 °C. Fractions of 300 μl were collected, and protein was methanol-precipitated before Western blotting with 6D11 and anti-flotillin-1 antibodies (BD Biosciences).

Cell Blotting—Measurement of cell surface protein was performed by cell blotting as previously described (21). Cells grown to confluence on glass coverslips were washed with Opti-MEM (Invitrogen) and then incubated on ice for 20 min with 6D11 (1:500 in Opti-MEM). Coverslips were then removed and placed face up on chromatography paper (Whatman No. 3MM) soaked in blotting buffer (0.5% sodium deoxycholate, 0.5% Nonidet-P40 in PBS). Nitrocellulose membranes (Bio-Rad) soaked in blotting buffer were placed on top of the coverslips, dry chromatography paper was placed on top of the membranes, and the sandwich was pressed together for 2 h. Membranes were probed with goat anti-mouse IgG to detect surface PrP or 6D11 followed by goat anti-mouse IgG to detect total PrP. Signals were revealed with Immobilon™ Western Chemiluminescent HRP substrate (Millipore) and visualized with a Bio-Rad XRS image scanner. Quantitative densitometry was done using the Quantity One software (Bio-Rad).

Detergent Insolubility—To assay protein aggregation by detergent insolubility, cells were resuspended in lysis buffer (0.5% sodium deoxycholate, 0.5% Nonidet-P40 in PBS) containing protease (cOmplete Mini EDTA-free, Roche Applied Science) and phosphatase (PhosSTOP, Roche Applied Science) inhibitor cocktails and incubated on ice for 20 min. Lysates were centrifuged for 5 min at 5000 × *g* to remove cell debris. Samples containing 1000 μg of protein in 500 μl were ultracentrifuged at 172,000 × *g* for 1 h at 4 °C. Insoluble proteins from

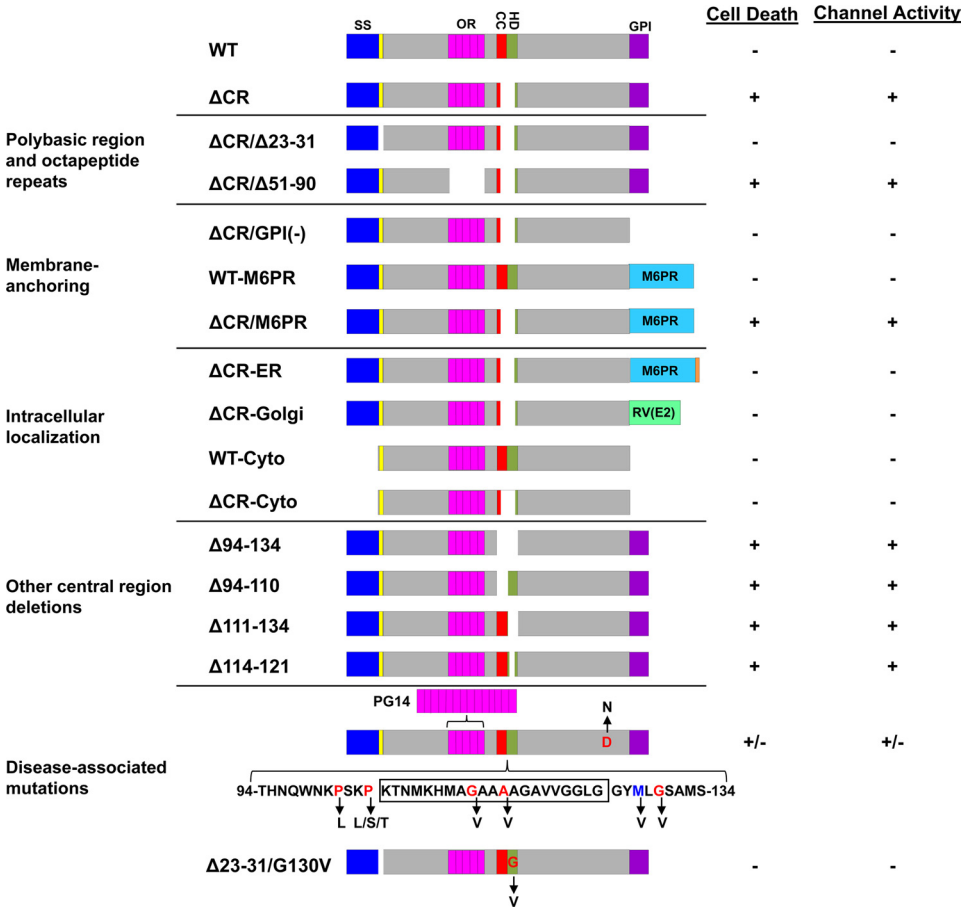

FIGURE 1. **Schematic of PrP constructs.** Structural domains of PrP are indicated by the colored blocks: signal sequence (*SS*, *blue*), residues 23–31 (*yellow*), octapeptide repeats (*OR*, *magenta*), charge cluster (*CC*, *red*), hydrophobic domain (*HD*, *green*), GPI signal sequence (*GPI*, *purple*). Cellular targeting domains include transmembrane segments from the M6PR (*blue*) and RV(E2) protein (*green*) and the ER retention signal KKMP (*orange*). Residues included in the central region (105–125) are indicated by the *boxed sequence in the lower schematic*. Residues representing disease-associated point mutations are *red*, and a non-pathogenic polymorphism (M128V) is *blue*. The presence or absence of activity in the DBCA (cell death) and patch clamp (ion channel) assays for each construct are indicated by pluses (+) or minuses (−) in the *right-hand columns*.

the pellet and soluble proteins methanol-precipitated from the supernatant were resuspended in equal volumes of SDS-PAGE loading buffer and analyzed by Western blotting.

RESULTS

In this study we modified the sequence of ΔCR PrP to remove several functionally important domains and to target the protein to specific cellular locations. We also introduced additional deletion and point mutations into the central region. The constructs analyzed are summarized in Fig. 1. Each molecule was expressed in clones of stably transfected HEK cells, and its expression level and cellular localization were determined. We then tested the activity of each construct using the DBCA and whole-cell patch clamping. The DBCA measures the susceptibility of the cells to killing by the aminoglycoside antibiotic, G418, which is greatly enhanced by expression of ΔCR PrP (7). Cells were treated for 24 h with G418 and then assayed for cell viability by MTT reduction. For whole-cell patch clamping, cells were held for approximately 10 min at a potential of −80 mV, and the percentage of time during which spontaneous currents exceeded 450 pA was determined. Under these conditions, ΔCR PrP induces large fluctuating inward currents in transfected cells (9). For each of the constructs, three independent HEK cell clones were analyzed with similar results, and data for one set of representative clones are shown here.

The N-terminal Polybasic Domain, but Not the Octapeptide Repeats, Is Necessary for ΔCR PrP Toxicity—Although the structure of the flexible, N-terminal half of PrP^C (amino acids 23–123) lacks observable secondary structure by NMR and x-ray crystallography (22, 23), it does contain several regions of known biological function. Residues 23–31 have been implicated in endocytosis of PrP via clathrin-coated pits, binding to glycosaminoglycans (GAGs), and protein transduction across lipid bilayers (24–27). Amino acids 51–90 encompass five octapeptide repeats that bind copper ions and are necessary for copper-induced endocytosis (28, 29).

To determine whether these two N-terminal domains are involved in ΔCR PrP toxicity, we deleted residues 23–31 or 51–90 to obtain ΔCR/Δ23–31 and ΔCR/Δ51–90 PrP (Fig. 1). By Western blotting, ΔCR/Δ23–31 and ΔCR/Δ51–90 PrP showed glycosylation patterns similar to those of WT and ΔCR PrP. Both proteins migrated as three bands corresponding to di-, mono-, and unglycosylated molecules, although the molecular sizes of each of the glycoforms was smaller as a result of the additional deletions (Fig. 2*A*, *lanes 2–5*). In all the clones exam-

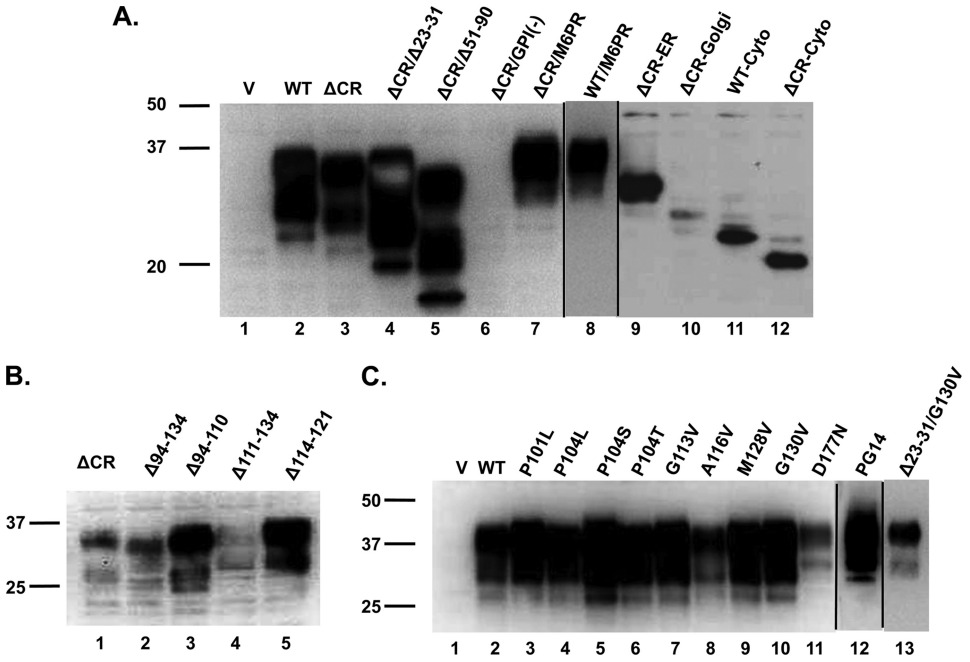

FIGURE 2. **PrP expression levels.** Western blots show PrP expression levels of each of the constructs in HEK cell clones using antibodies 6D11 (*A* and *C*) or 6H4 (*B*). Samples were normalized for total protein by BCA before loading. Molecular size markers are given in kDa. *V*, vector.

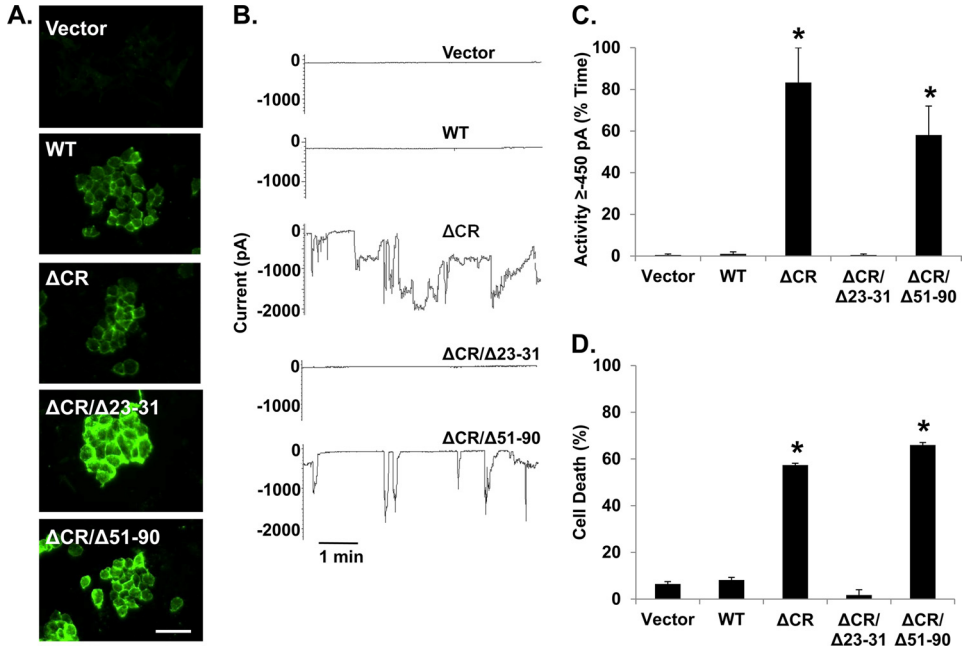

FIGURE 3. **The N-terminal polybasic domain, but not the octapeptide repeats, is necessary for ΔCR toxicity.** *A*, surface immunofluorescence staining of PrP on HEK cells stably expressing WT, ΔCR, ΔCR/Δ23–31, or ΔCR/Δ51–90 PrP or empty vector is shown. *Scale bar* = 50 μm. *B*, whole-cell patch clamp recordings at −80 mV were made from cells expressing the indicated constructs. *C*, shown is quantitation of the currents recorded in *panel B*, plotted as the percentage of total time the cells exhibited an inward current ≥450 pA (mean ± S.E., $n = 5$ cells). *D*, cell death induced by G418 treatment (400 μg/ml) measured by MTT reduction (mean ± S.E., $n \geq 10$ wells from three independent experiments). *Asterisks* (*) indicate values that are significantly greater than those for WT PrP ($p < 0.05$, one-tailed Student's *t* test).

ined ΔCR/Δ23–31 PrP had higher levels of expression than WT PrP, most likely due to decreased endocytosis and degradation (27). Immunofluorescence staining showed similar surface localization patterns for ΔCR/Δ23–31, ΔCR/Δ51–90, WT, and ΔCR PrP (Fig. 3*A*).

Analysis of ΔCR/Δ51–90 PrP-expressing cells by DBCA and whole-cell patch clamping revealed levels of cell death and spontaneous inward currents, respectively, that were similar to those observed for ΔCR PrP and significantly higher than for WT PrP (Fig. 3, *B–D*). In contrast, no significant increase in cell death or induction of spontaneous currents was detected in ΔCR/Δ23–31 PrP-expressing cells compared with those expressing WT PrP. Collectively, these results demonstrate that the N-terminal polybasic domain, but not the octapeptide repeats, is necessary for the toxicity of ΔCR PrP.

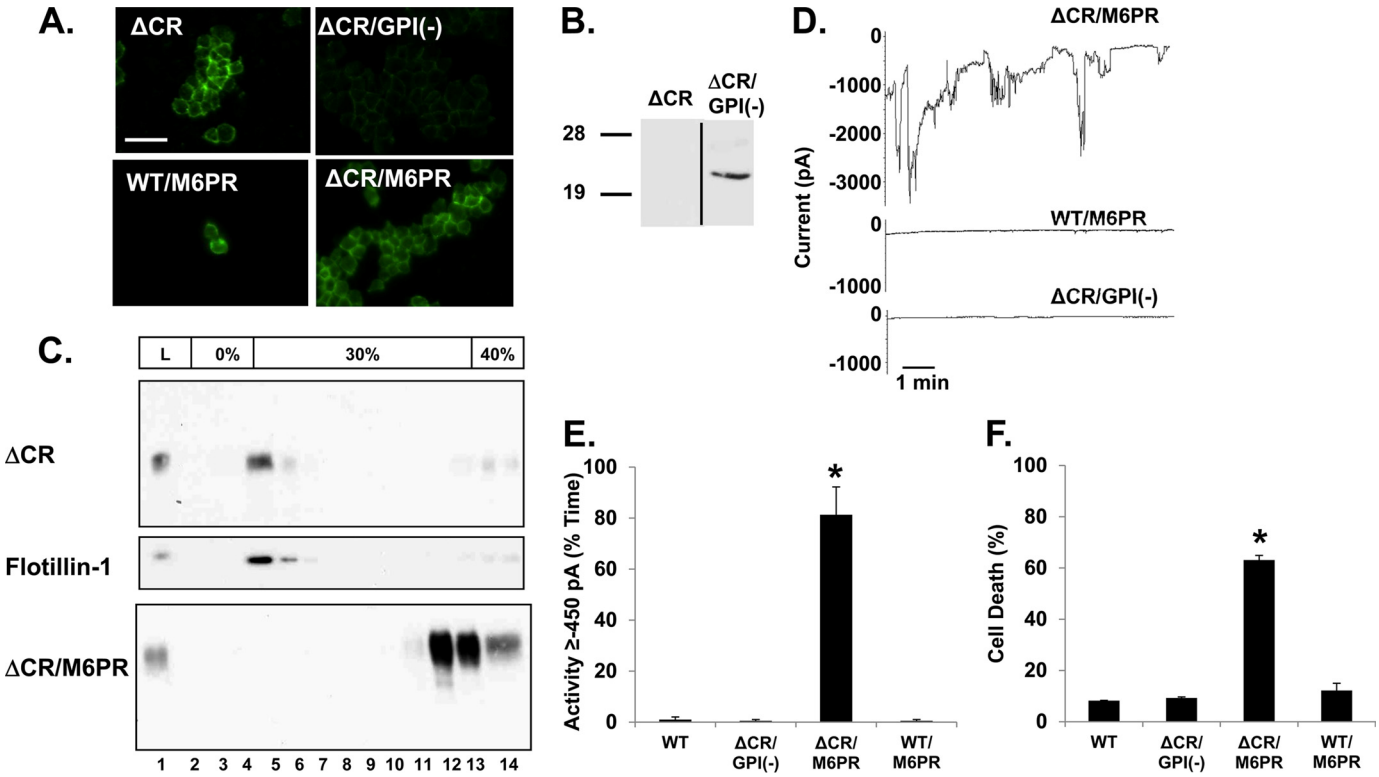

FIGURE 4. **Membrane attachment, but not lipid raft localization, is necessary for ΔCR PrP toxicity.** *A*, shown is surface immunofluorescence staining of PrP on HEK cells stably expressing ΔCR, ΔCR/GPI(−), ΔCR/M6PR, or WT/M6PR. *Scale bar* = 50 μm. *B*, a Western blot detects PrP secreted into the growth medium by cells expressing ΔCR and ΔCR/GPI(−) PrP. *C*, an Opti-Prep gradient to separate DRMs is shown. ΔCR PrP is present at the 0/30% Opti-Prep interface (*lanes 4–5*), as is the DRM marker flotillin-1. ΔCR/M6PR PrP is present in the fractions containing 40% Opti-Prep (*lanes 12–14*). Sample from the total cell lysate (*L*) is shown in *lane 1*. *D*, whole-cell patch clamp recordings at −80 mV were made from cells expressing the indicated constructs. *E*, quantitation of the currents recorded in *panel D* plotted as the percentage of total time the cells exhibited an inward current ≥450 pA (mean ± S.E., $n = 5$ cells). *F*, cell death induced by G418 treatment (400 μg/ml) measured by MTT reduction (mean ± S.E., $n \geq 10$ wells from three independent experiments). *Asterisks* (*) indicate values that are significantly greater than those for WT PrP ($p < 0.05$, one-tailed Student's *t* test).

Membrane Attachment, but Not Lipid Raft Localization, Is Necessary for ΔCR Toxicity—PrP^C associates with the outer leaflet of the plasma membrane via a C-terminal glycosylphosphatidylinositol (GPI) anchor, and most molecules are localized to lipid rafts (defined biochemically as detergent-resistant membranes) (30, 31). To determine whether membrane attachment is necessary for ΔCR PrP toxicity, we deleted the GPI attachment signal (amino acids 231–254) to obtain ΔCR/GPI(−) PrP (Fig. 1). Most of this construct was secreted into the medium in a predominantly unglycosylated form, as detected by Western blotting of proteins collected from the medium by methanol precipitation (Fig. 4*B*), similar to what was observed by Chesebro *et al.* (32). In contrast, very little of the protein remained cell-associated, as detected by Western blotting of the cell lysates (Fig. 2*A*, *lane 6*) or by cell surface immunofluorescence staining (Fig. 4*A*). Analyses by DBCA and whole-cell patch clamping of cells expressing ΔCR/GPI(−) PrP revealed levels of cell death and spontaneous inward currents similar to those of WT PrP expressing cells and significantly lower than those of ΔCR PrP-expressing cells (Figs. 4*D–F*).

To test whether the type of membrane attachment is important, we replaced the endogenous GPI anchor attachment signal with the transmembrane domain of the M6PR to obtain ΔCR/M6PR and WT/M6PR PrP (Fig. 1) (14). These molecules were glycosylated (Fig. 2*A*, *lanes 7* and *8*) and localized to the cell surface (Fig. 4*A*). To determine whether localization to lipid rafts was affected by replacement of the GPI anchor with a transmembrane domain, we fractionated cell extracts on an Opti-Prep density gradient (Fig. 4*C*). In contrast to ΔCR PrP, which co-fractionated with the DRM resident protein flotilin-1 at the 0–30% interface, ΔCR/M6PR PrP remained at the bottom of the gradient with the densest fractions. This result demonstrates that, as expected, ΔCR/M6PR PrP does not localize to lipid rafts like ΔCR PrP. Cells expressing ΔCR/M6PR PrP, but not WT/M6PR PrP, displayed drug hypersensitivity and spontaneous currents that were similar to those of ΔCR PrP-expressing cells and significantly higher than those of WT PrP-expressing cells (Fig. 4, *D–F*). Taken together, these results indicate that membrane attachment, but not lipid raft localization, is required for ΔCR PrP toxicity. However, either transmembrane or GPI anchoring is sufficient for activity.

Localization to the Cell Surface Is Required for ΔCR Toxicity—We next wanted to determine whether ΔCR PrP toxicity requires residence on the cell surface or whether molecules targeted to intracellular compartments can also be toxic. To restrict expression to the ER, the retention motif KKMP was added to the C terminus of ΔCR/M6PR to obtain ΔCR-ER PrP (33) (Fig. 1). To localize expression to the Golgi, the GPI signal was replaced by a transmembrane domain from the rubella virus envelope glycoprotein E2 to obtain ΔCR-Golgi PrP (15) (Fig. 1).

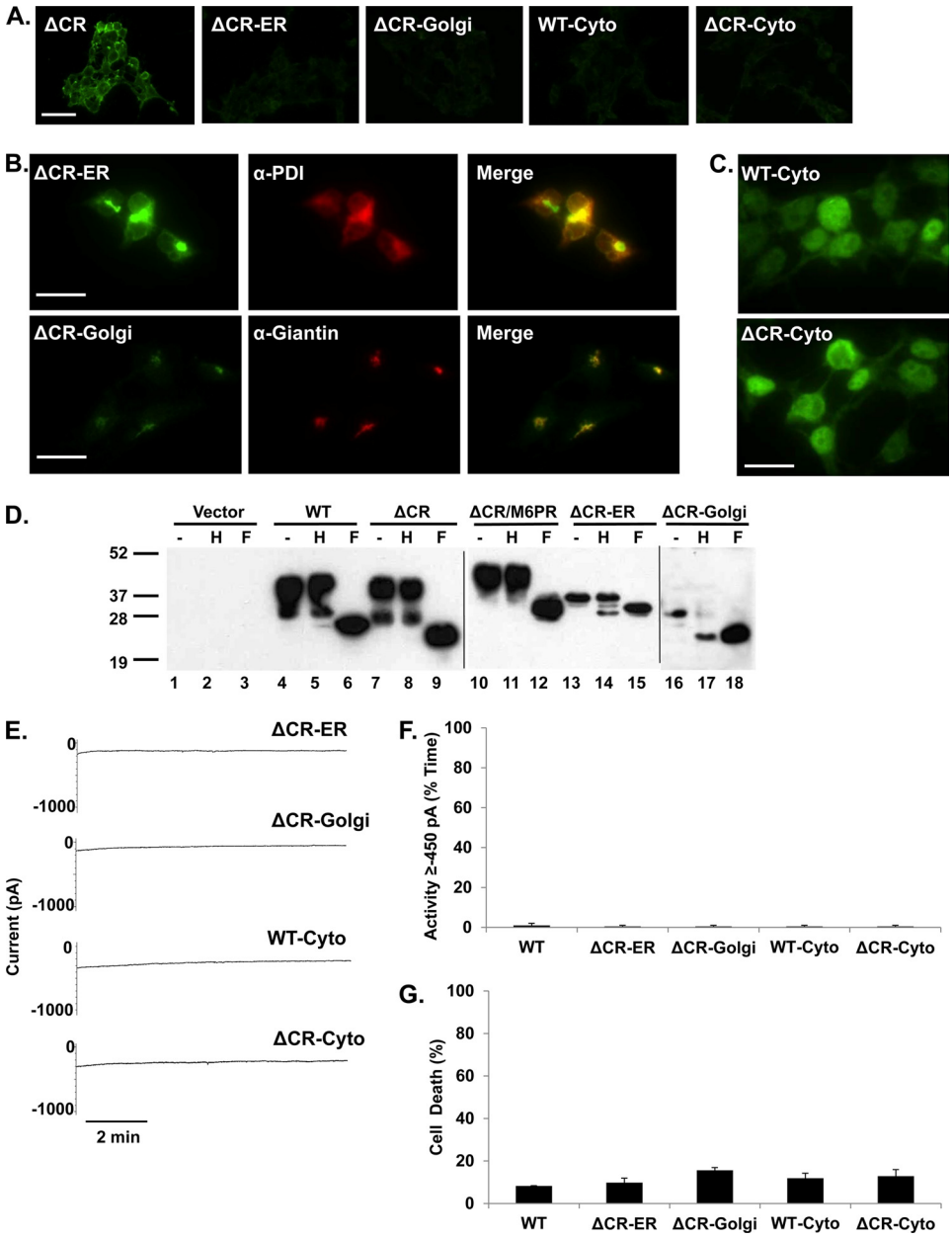

FIGURE 5. **Localization to the plasma membrane is required for ΔCR toxicity.** *A*, surface immunofluorescence staining of PrP on HEK cells stably expressing ΔCR, ΔCR-ER, ΔCR-Golgi, WT-Cyto, or ΔCR-Cyto PrP is shown. *Scale bar* = 50 μm. *B* and *C*, staining of permeabilized cells for PrP (*green*), protein disulfide isomerase (*PDI*; *red*), and giantin (*red*) is shown, with regions of colocalization shown in *yellow* in the merged images. *Scale bars* = 20 μm. *D*, Western blots of untreated (−), endoglycosidase H-treated (*H*), or *N*-glycosidase F-treated (*F*) cell lysates are shown. *E*, whole-cell patch clamp recordings at −80 mV were made from cells expressing the indicated constructs. *F*, quantitation of the currents recorded in *panel E* are plotted as the percentage of total time the cells exhibited inward a current ≥450 pA (mean ± S.E., $n = 5$ cells). *G*, cell death was induced by G418 treatment (400 μg/ml) measured by MTT reduction (mean ± S.E., $n \geq 10$ wells from 3 independent experiments). No statistically significant differences in cell death or inward currents were observed between any of these mutants and WT PrP.

To verify the predicted localization patterns of these constructs, we performed immunofluorescence staining and tested maturation of *N*-linked oligosaccharide chains by glycosidase digestion. As expected, neither ΔCR-ER nor ΔCR-Golgi PrP was present on the cell surface (Fig. 5*A*). Immunofluorescence staining of permeabilized cells revealed co-localization of ΔCR-ER PrP with the ER marker protein disulfide isomerase (*PDI*) (Fig. 5*B*). ΔCR-Golgi PrP, in contrast, co-localized with the Golgi marker giantin in a discrete spot near the nucleus. Western blots of endoglycosidase H-treated cell lysates revealed a shift in migration for both ΔCR-ER and ΔCR-Golgi PrP. In contrast, WT, ΔCR, and ΔCR/M6PR PrP were completely insensitive to digestion (Fig. 5*D*). Some glycosylated ΔCR-ER and ΔCR-Golgi remained after endoglycosidase H treatment, suggesting either incomplete cleavage or trafficking of a fraction of the molecules beyond the mid-Golgi. However, both molecules migrated faster than fully mature WT PrP before digestion, consistent with incomplete oligosaccharide maturation. Taken together, these data indicate that ΔCR-ER and ΔCR-Golgi PrP are localized to the predicted intracellular compartments. Although the level of ΔCR-ER PrP expression is slightly lower than that of WT PrP, ΔCR-Golgi is expressed at

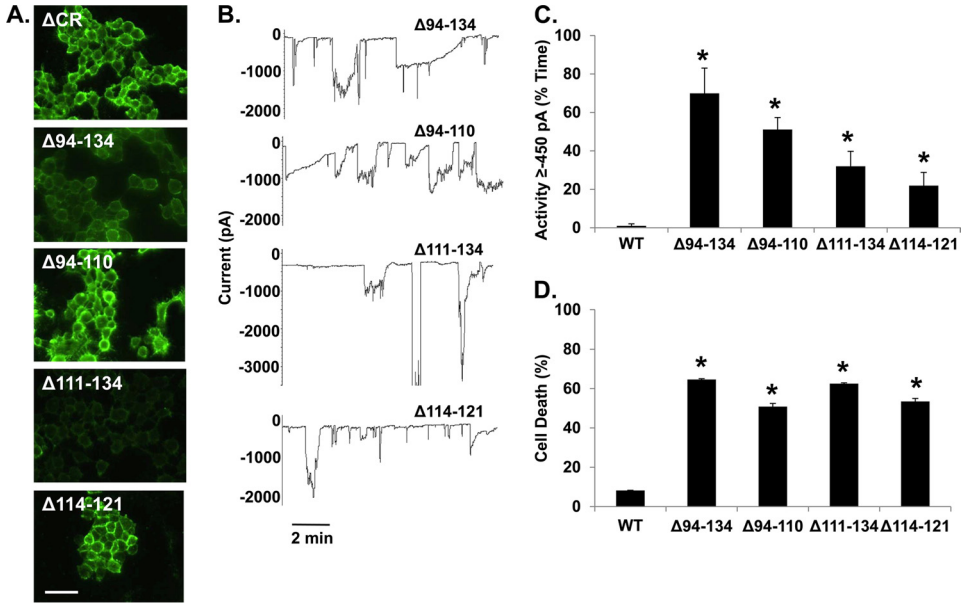

FIGURE 6. **Deletion of charged or hydrophobic residues in the central region causes toxicity.** *A*, shown is surface immunofluorescence staining of PrP on HEK cells stably expressing Δ94–134, Δ94–110, Δ111–134, or Δ114–122 PrP. *Scale bar* = 50 μm. *B*, whole-cell patch clamp recordings at −80 mV were made from cells expressing the indicated constructs. *C*, quantitation of the currents recorded in *panel B* are plotted as the percentage of total time the cells exhibited an inward current ≥450 pA (mean ± S.E., $n = 5$ cells). *D*, cell death induced by G418 treatment (400 μg/ml) was measured by MTT reduction (mean ± S.E., $n \geq 10$ wells from 3 independent experiments). *Asterisks* (*) indicate values that are significantly greater than those for WT PrP ($p < 0.05$, one-tailed Student's *t* test).

much lower levels by Western blotting (Fig. 2*A*, *lanes 9* and *10*). Based on immunofluorescence staining, however, the amount of ΔCR-Golgi localized to the Golgi is similar to that for WT and ΔCR PrP (data not shown).

ΔCR-ER and ΔCR-Golgi PrP failed to induce significantly higher levels of cell death or spontaneous current than WT PrP (Fig. 5, *E–G*). Because ΔCR-ER and ΔCR-Golgi PrP (as well as WT-Cyto and ΔCR-Cyto PrP; see below) were expressed at significantly lower levels than WT and ΔCR PrP, we also examined the toxicity of a ΔCR PrP clone with an expression level similar to that of ΔCR-Golgi, our lowest expressing construct (supplemental Fig. S1*A*). We found that the low-expressing ΔCR clone had significantly more drug-induced cell death than the WT or ΔCR-Golgi clones, indicating that the lack of toxicity of the ER, Golgi, and cytoplasmic constructs was due to altered localization rather than level of expression (supplemental Fig. S1*B*). Therefore, we conclude that localization at the cell surface is required for ΔCR PrP toxicity and that molecules residing in the ER or Golgi are not toxic.

Cytoplasmic PrP Is Not Toxic—Previous reports have associated accumulation of PrP in the cytoplasm due to inefficient translocation or retro-translocation with cytotoxicity (34). We, therefore, decided to test whether PrP expressed in the cytoplasm could exert toxicity measurable in our assays. To target the proteins to the cytoplasm, we deleted the endogenous signal sequence (PrP 1–22) and GPI attachment motif (232–254) from both WT and ΔCR to obtain WT-Cyto and ΔCR-Cyto PrP (Fig. 1). As expected for proteins that do not enter the secretory pathway, these molecules lacked glycosylation (Fig. 2*A*, *lanes 11* and *12*). Expression levels of both constructs were lower than for WT PrP, probably due to proteasomal degradation (35). Immunofluorescence staining revealed that both molecules were absent from the cell surface and localized entirely in the cytoplasm (Fig. 5, *A* and *C*). Both WT-Cyto and ΔCR-Cyto PrP failed to induce significantly higher levels of cell death or spontaneous currents than WT PrP (Fig. 5, *E–G*). This result indicates that ΔCR PrP must be attached to the plasma membrane to exert its toxicity and that cytoplasmically localized molecules are not toxic.

Deletion of Charged or Hydrophobic Residues in the Central Region Causes Toxicity—The 105–125 region, deleted in ΔCR PrP, includes a cluster of positively charged amino acids (105–111) and a highly conserved stretch of hydrophobic residues (112–125). To determine whether deletion of the charged or hydrophobic amino acids is responsible for ΔCR PrP toxicity, we analyzed several deletions previously expressed in transgenic mice (36, 37). Δ94–134 eliminates both the charged and hydrophobic residues, Δ94–110 eliminates just the charged residues, Δ111–134 eliminates all of the hydrophobic residues, and Δ114–121 eliminates part of the hydrophobic domain (Fig. 1). All four of these PrP molecules showed normal glycosylation (Fig. 2*B*, *lanes 2–5*) and localization to the cell surface (Fig. 6*A*). Cells expressing all of these constructs displayed significantly higher levels of cell death and inward current activity than cells expressing WT PrP (Figs. 6, *B–D*). Thus, we conclude that disruption of either the cluster of positively charged amino acids or the hydrophobic domain triggers PrP cytotoxicity. Because the Δ94–110 and Δ114–121 constructs were expressed at substantially higher levels than the other deletion mutants (Fig. 2*B*, *lanes 2–5*) yet showed comparable or lower activity in our assays (Fig. 6, *C* and *D*), these molecules may be less potent in terms of their intrinsic toxicity.

Disease-associated Mutations Within and Flanking the CR Cause Toxicity—Because deletions of either charged or hydrophobic amino acids in the central region produce toxicity, we sought to determine whether similar effects were produced by dominantly inherited point mutations within this domain that are associated with familial prion diseases of humans (Fig. 1).

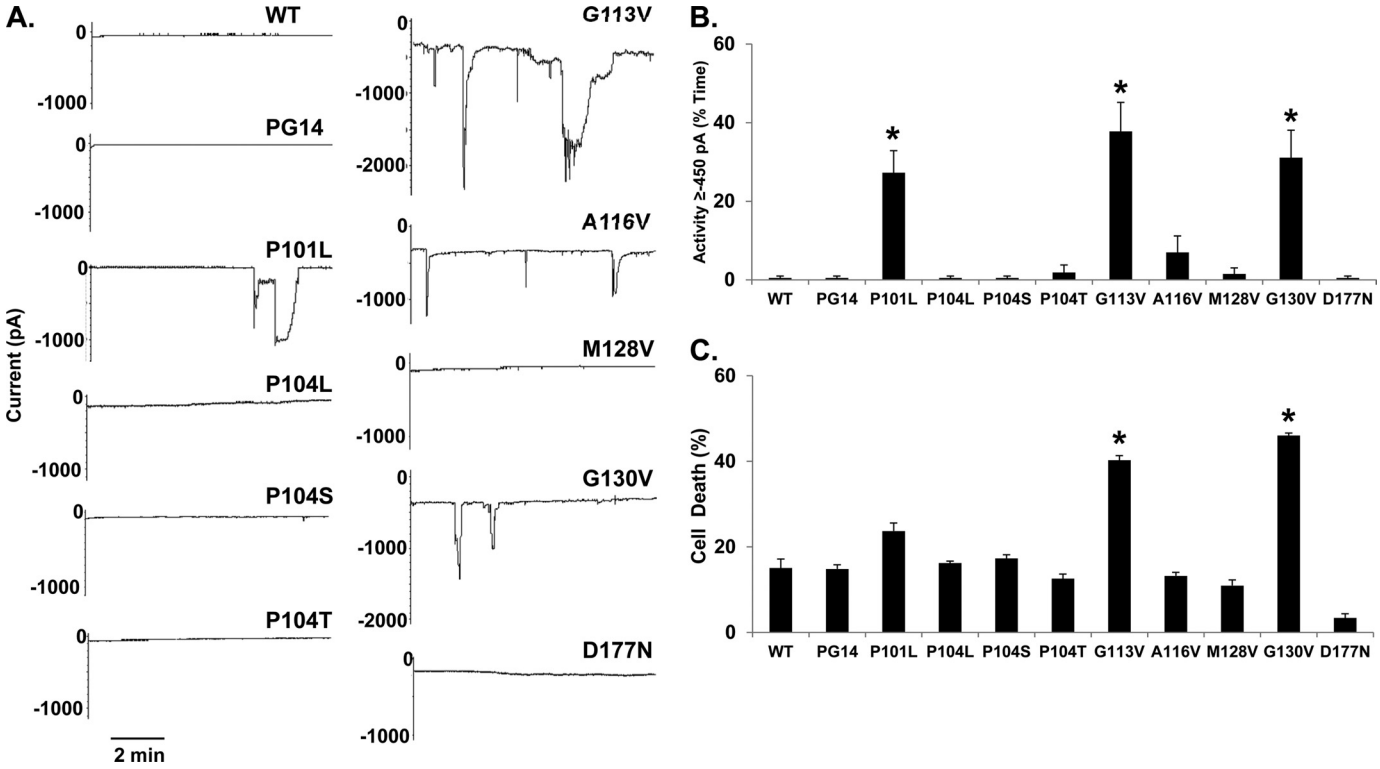

FIGURE 7. **Pathogenic mutations within and flanking the CR cause toxicity.** *A*, whole-cell patch clamp recordings at −80 mV were made from cells expressing WT, PG14, P101L, P104L, P104S, P104T, G113V, A116V, M128V, G130V, or D177N PrP. *B*, quantitation of the currents recorded in *panel A* are plotted as the percentage of total time the cells exhibited an inward current ≥450 pA (mean ± S.E., $n = 5$ cells). *C*, cell death induced by G418 treatment (400 μg/ml) was measured by MTT reduction (mean ± S.E., n ≥ 10 wells from 3 independent experiments). *Asterisks* (*) indicate values that are significantly greater than those for WT PrP ($p < 0.05$, one-tailed Student's *t* test).

We previously observed the generation of ΔCR PrP-like currents in cells expressing P101L, G113V, and G130V mutants (9). Here we extended those findings by examining additional point mutations in the CR (P104L, P104S, P104T, and A116V). For comparison, we also analyzed two pathogenic mutations outside of the central region; that is, a nine-octapeptide insertional mutation in the N terminus (referred to as PG14) and a point mutation (D177N) in the C terminus. As a negative control, we also tested a non-pathogenic polymorphism (M128V). All these mutants showed normal glycosylation patterns and, with the exception of A116V and D177N, comparable expression levels (Fig. 2*C*). The latter two mutants showed lower expression levels, possibly due to increased protein turnover.

Whole-cell patch clamp of cells expressing the P101L, G113V, and G130V mutants revealed a significantly higher level of spontaneous currents than cells expressing WT PrP, as previously reported (Figs. 7, *A* and *B*). DBCA detected a significantly higher amount of cell death in G113V- and G130V-expressing cells and a slightly higher but not statistically significant level for P101L-expressing cells (Fig. 7*C*). P104L, P104S, P104T, A116V, D177N, and PG14 PrPs did not produce significantly increased levels of cell death or spontaneous currents compared with WT PrP. In both assays, the active pathogenic mutants showed a smaller effect than ΔCR PrP ($p < 0.05$, one-tailed Student's *t* test). Because some disease-associated mutations impair delivery of PrP to the cell surface (38, 39) and because cell surface expression is important for ΔCR PrP toxicity, we investigated the cell surface localization of the PrP point mutants. By immunofluorescence staining, all of the mutant PrPs were detectable at the cell surface with the exception of PG14, which has been previously shown to accumulate intracellularly (Fig. 8*A*) (38). To quantitate more precisely the surface expression of each mutant, a cell blotting assay was used. In this assay the amount of surface-exposed PrP accessible to antibody binding was compared with the total amount of PrP (21). We found that the three active mutants (P101L, G113V, and G130V) had surface PrP levels similar to those of WT, whereas three inactive mutants (PG14, A116V, and D177N) displayed significantly reduced surface expression (Fig. 8*B*). However, three other inactive mutants (P104L, P104S, and P104T) were expressed normally on the cell surface. Overall, there was no significant correlation between cell death in the DBCA and levels of cell surface PrP (Fig. 8*D*). Thus, although cell surface expression is necessary for toxicity in our assays, a lack of surface expression cannot explain the lack of activity of several of the point mutants.

We wondered whether the lack of toxicity of some of the mutants was due to the fact that they were aggregated. To test this hypothesis, we measured insolubility of the mutants by ultracentrifugation. PG14, P104S, G130V, and D177N were found to have significantly higher proportions of insoluble molecules than WT PrP (Fig. 8*C*). Of these four mutants, one (G130V) had significant activity by DBCA and whole-cell patch clamping, whereas the others were inactive. Thus, there was no correlation between aggregation and activity in the two assays

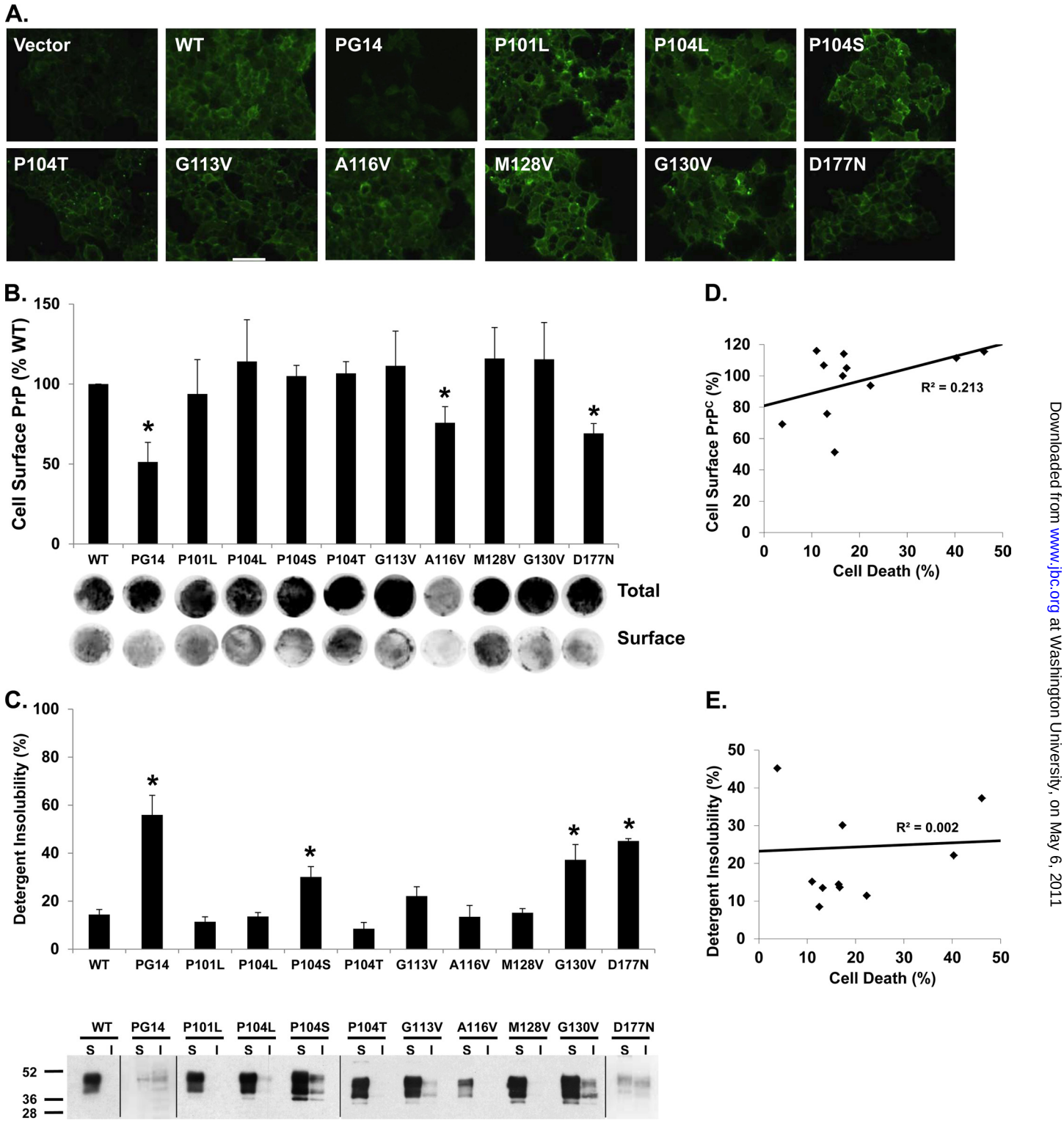

FIGURE 8. **Cellular localization and aggregation of disease-associated mutants.** *A*, shown is surface immunofluorescence staining of PrP on HEK cells stably expressing WT, PG14, P101L, P104L, P104S, P104T, G113V, A116V, M128V, G130V, or D177N PrP or empty vector. *Scale bar* = 50 μm. *B*, shown is quantitation of cell surface PrP for each of the mutants (mean ± S.E., $n = 3$ independent experiments) by cell blotting. Examples of total and surface signals are shown below each bar. *C*, quantitation of the percentage of insoluble PrP (mean ± S.E., $n = 3$ independent experiments) is shown. Western blots of PrP in detergent-soluble (*S*) and insoluble (*I*) fractions are shown *below each bar*. *Asterisks* (*) indicate values that are significantly greater than those for WT PrP ($p < 0.05$, one-tailed Student's *t* test). Plots of cell death *versus* cell surface PrP (*D*) or cell death *versus* detergent insolubility (*E*) for each disease-associated point mutant show no significant correlations.

(Fig. 8*E*). These results demonstrate that aggregation neither induces nor prevents toxicity in our cell assays.

To determine whether the N-terminal polybasic domain was essential for the toxicity of the disease-associated point mutations, as it is for ΔCR, we deleted amino acids 23–31 in G130V to create Δ23–31/G130V (Fig. 1). This molecule was expressed at levels comparable levels to G130V with an intact N terminus (Fig. 2*C*, *lanes 10* and *13*) and showed a similar surface localiza-

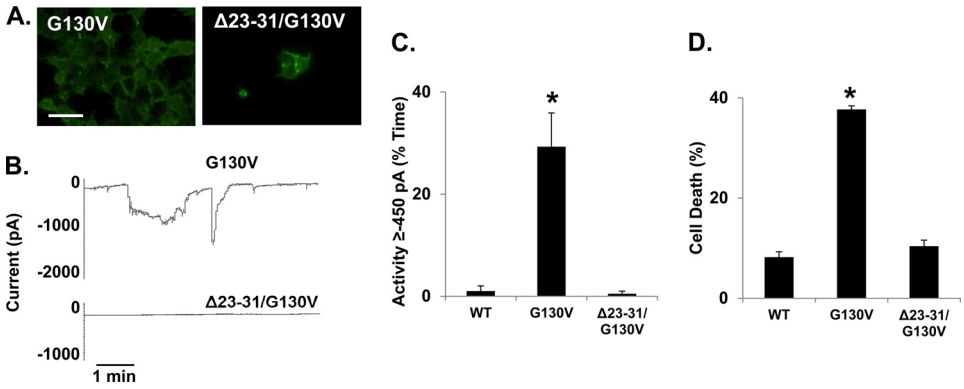

FIGURE 9. **The N-terminal polybasic domain is necessary for toxicity of the disease-associated point mutant G130V.** *A*, surface immunofluorescence staining of PrP on HEK cells stably expressing G130V or Δ23–31/G130V PrP is shown. *Scale bar* = 50 μm. *B*, whole-cell patch clamp recordings at −80 mV is shown. *C*, shown is quantitation of the currents recorded in *panel B*, plotted as the percentage of total time the cells exhibited inward current ≥450 pA (mean ± S.E., $n = 5$ cells). *D*, cell death induced by G418 treatment (400 μg/ml) is measured by MTT reduction (mean ± S.E., $n \geq 10$ wells from 3 independent experiments). *Asterisks* (*) indicate values that are significantly greater than those for WT PrP ($p < 0.05$, one-tailed Student's *t* test).

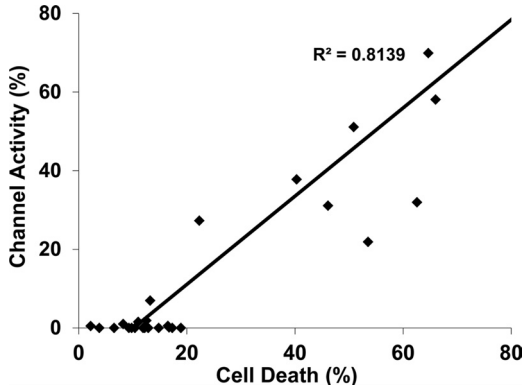

FIGURE 10. **Correlation between G418-induced cell death and ion channel activity.** Levels of cell death and ion channel activity were plotted for each PrP molecule in this study. The linear regression line denotes significant correlation between the two assays ($p < 0.0005$, one-tailed Student's *t* test).

tion pattern (Fig. 9*A*). Unlike G130V, Δ23–31/G130V PrP did not induce spontaneous currents or significantly increase cell death (Figs. 9, *B–D*). Thus, deleting amino acids 23–31 in either ΔCR or G130V eliminates activity in our assays, suggesting that both point mutations and deletions in the central region depend on the N-terminal polybasic region for toxicity.

Drug Hypersensitivity and Channel Activity Correlate with Each Other—Because we performed the same two assays on all mutant constructs, we wondered whether the outputs of these assays were correlated with each other. We found a strong, positive correlation ($R^2 = 0.8139$) ($p < 0.0005$, one-tailed Student's *t* test) between the activities measured in the DBCA and in whole-cell patch clamp (Fig. 10), suggesting that these two assays are both detecting the consequences of a common molecular event triggered by toxic PrP molecules.

DISCUSSION

Although much is known about the infectivity of prions, the mechanisms underlying their neurotoxicity remain unclear. It is known that structural changes occur during the transition from PrP^C to PrP^{Sc}, notably in the central region of the protein (40, 41), but how these changes are related to prion toxicity remains to be determined. Deleting parts of the central region of PrP causes spontaneous neurodegeneration in transgenic mice, a phenomenon that may provide clues to the toxic pathways triggered by PrP^{Sc}. We previously reported that cells expressing ΔCR PrP, which is missing amino acids 105–125, exhibit spontaneous ionic currents and hypersensitivity to certain cationic drugs. In the present study we have utilized assays based on these two phenomena to determine which regions of PrP are necessary for activity and which cellular compartments are involved.

Residues 23–31 Are Essential for PrP Activity—We have found that deletion of residues 23–31 abolishes both the ion channel and drug sensitizing activities of ΔCR and G130V PrP. Although there is no detectable secondary structure in the N-terminal half of PrP^C based on NMR analysis (22), this region has been found to mediate several functional attributes of PrP^C and to bind several putative ligands. For example, residues 23–31 are essential for clathrin-mediated endocytosis. However, we have found that point mutations in this region that eliminate endocytosis do not affect ΔCR PrP toxicity,[4] suggesting that toxicity is not dependent on endocytosis. Instead, this region may be important for the interaction of PrP with other molecules, including proteins, GAGs, or lipids. In fact, residues 23–31 constitute 1 of 3 GAG binding sites on PrP^C (24, 25). We have previously reported that application of an exogenous GAG (pentosan polysulfate) rapidly abolishes ΔCR PrP-induced currents, an effect that may be due to binding of pentosan polysulfate to the 23–31 region (9). Residues 23–27 (KKRPK) have also been shown to function as a protein transduction domain, similar to an analogous sequence in the HIV Tat protein that is capable of translocating extracellular polypeptides into the cytoplasm (26). Interestingly, this process is dependent on binding to cell-surface GAGs. In what may be a related phenomenon, the same N-terminal residues have also been shown to possess a bactericidal activity based on the ability of recombinant PrP to induce leakage of bacterial membranes (42). Taken together, these observations suggest a model whereby the 23–31 region acts a tethered protein transduction domain that allows PrP to transiently span the lipid bilayer, thereby forming a channel or pore. In WT PrP, channel formation may be minimized by the presence of the hydrophobic segment (res-

[4] L. Westergard, J. A. Turnbaugh, and D. A. Harris, submitted for publication.

idues 111–135), whereas deletion or mutation of this segment (as in ΔCR and related molecules) would enhance channel-forming activity.

Another functionally important region in the N-terminal tail of PrP is the octapeptide repeat domain (residues 51–90). These residues bind copper and other transition metals, leading to endocytic uptake of PrP^C, due to re-localization of PrP^C from lipid rafts into clathrin-coated pits via interactions with the low density lipoprotein receptor-related protein-1 (LRP1) (43). We found that the octapeptide repeats are dispensable for ΔCR PrP activity in our assays, arguing that metal binding is not necessary for these effects.

Cellular Locus of PrP Activity—One of the goals of this study was to determine the cellular site of ΔCR PrP toxicity. Therefore, we engineered the ΔCR PrP molecule to deliver it to cellular locations other than the plasma membrane, where it normally resides. Elimination of the GPI anchor, causing secretion into the medium, as well as deletion of the N-terminal signal sequence, resulting in cytoplasmic expression, abolished ΔCR PrP activity, arguing that membrane attachment is essential for activity. This conclusion is consistent with the observation that an anchorless form of Δ94–134 PrP does not induce spontaneous neurodegeneration in transgenic mice (44). Membrane tethering may facilitate a sustained interaction of the N-terminal, pore-forming region (residues 23–31) with the lipid bilayer. Alternatively, attachment to the membrane may be necessary to bring ΔCR PrP in close proximity to membrane-associated interacting proteins or GAGs. ΔCR PrP molecules that were targeted to the ER or Golgi lacked activity in our assays, suggesting that the protein needs to reside on the cell surface to exert its effects. Interestingly, a form of ΔCR PrP that was attached to the cell surface via a transmembrane domain rather than a GPI anchor was fully active, arguing that localization to lipid rafts is not required for activity.

Taken together with our previous observation that ΔCR PrP induces spontaneous currents in a variety of cell types, including those of both mammalian and insect origin, our data support the idea that the ΔCR PrP molecule itself forms non-selective, cation-permeable channels or pores in the plasma membrane (9). We are currently testing this hypothesis by attempting to reconstitute channel activity using recombinant forms of ΔCR PrP inserted into liposomes and artificial membranes. A less likely alternative is that ΔCR PrP activates a ubiquitously expressed, endogenous ion channel. There is evidence that PrP functionally and physically interacts with certain types of ionotropic glutamate receptors (45) and that neurons from PrP knock-out mice display several kinds of electrophysiological abnormalities (46–49). However, the nature of the interactions between PrP and endogenous ion channels remains unclear.

Disruption of the Central Region Induces PrP Toxicity—Several different deletions spanning the central region of PrP have been shown to induce a spontaneous neurodegenerative phenotype when expressed in transgenic mice (10, 36, 37, 50). We showed previously that one of these, Δ32–134, was active in the DBCA, although its potency was less than that of ΔCR, correlating with a less aggressive phenotype in mice (7). Here, we assayed the activity of several additional deletion mutants in the central region, including Δ94–134, Δ111–134, Δ94–110, and Δ114–121. All four of these mutants displayed activity in both the DBCA and patch clamp assays. Collectively, our results show that deleting either the charge cluster or the hydrophobic domain can trigger PrP cytotoxicity. Of note, the Δ94–134 and Δ111–134 constructs have been shown to cause neurodegeneration in transgenic mice, whereas Δ94–110 and Δ114–121 constructs do not (36, 37). For the latter mutant, the lack of a neurodegenerative phenotype may be due to low expression levels in the transgenic line analyzed. It is also possible that Δ94–110 and Δ114–121 molecules are intrinsically less toxic, a conclusion suggested by the lower activity of these mutants in our assays when normalized to expression levels.

Although the molecular consequences of disrupting the central region remain to be determined, one possible explanation for our results is that this region represents a binding site for a ligand such as stress-inducible protein 1 or vitronectin (51, 52) that influences cell survival or neuroprotection. The absence of ligand binding may then result in impaired viability. Alternatively, these deletions may influence membrane insertion of the hydrophobic domain, for example, reducing the amount of transmembrane PrP (^{Ctm}PrP) that is formed (53, 54).

Disease-associated Mutations—Although the majority of prion disease cases are sporadic in origin, 15% are familial and are linked to dominantly inherited point or insertional mutations in the gene encoding PrP (55). Some of these mutants produce a relatively soluble, protease-sensitive form of PrP that is likely to be neurotoxic via non-PrP^{Sc}-dependent pathways (56–58). We have undertaken a comprehensive analysis of all the single amino acid point mutations that have been described that lie within or near the central region, including P101L, P104L/S/T, G113V, A116V, and G130V (mouse PrP numbering). All of these mutations have been associated with Gerstmann-Sträussler-Scheinker (GSS) syndrome, with the exception of G113V, which is associated with a Creutzfeldt-Jakob Disease (CJD) phenotype (55). We also examined two mutations outside of the central region; that is, a 9-octapeptide insertion (PG14) associated with a mixed GSS/CJD phenotype and D177N, associated with familial CJD. As a negative control, we also analyzed the non-pathogenic polymorphism M128V.

Three of the point mutants, P101L, G113V, and G130V, exhibited significant activity in the DBCA and patch clamp assays but less than that of ΔCR PrP. The lower potency of P101L *in vitro* correlates with the less severe phenotype produced by this mutant in transgenic mice (10, 59). Conversely, the G113V mutation, the most potent in our cell assays, is associated with a very early onset of disease in humans (60).

To explain why some of the CR mutants (P104L/S/T and A116V) were inactive in our assays, we tested the solubility and cellular localization of the mutants with the idea that molecules that were highly aggregated or retained intracellulary would not be capable of inducing ion channels or drug hypersensitivity. However, we did not observe a correlation between solubility and activity in our assays, with one of the three active mutants (G130V) showing significantly decreased solubility, and three of the inactive mutants displaying solubility similar to that of WT PrP. Similarly, there was no correlation between cell surface localization and activity. Only one of the four inactive

mutants (A116V) was present in significantly reduced levels on the cell surface. Based on these results, we conclude that neither cellular mislocalization nor aggregate formation explains the lack of activity of the P104L/S/T and A116V mutants. These mutants may have an activity that lies below the threshold of detectability in our assays, or they may be toxic via mechanisms that are unrelated to enhanced ion channel activity.

Relationship between Channel Activity and Drug Hypersensitivity—We observed a striking correlation between the channel-inducing and G418-sensitizing activities of the different PrP constructs (Fig. 10). Mutants that display significant ion channel activity are the same as those that render cells hypersensitive to G418, whereas mutants that lack channel activity have no effect on drug sensitivity. This correlation strongly suggests a mechanistic relationship between the ion channel and drug sensitivity phenotypes. One possible scenario is that the ion channels activated by ΔCR PrP are permeable to the drugs and allow increased cytoplasmic accumulation of these toxic compounds. Consistent with this idea, there is evidence that aminoglycoside antibiotics can permeate some cation-selective channels (61–63). An alternative possibility is that ion channel activation enhances other cellular processes responsible for drug uptake. For example, ion influx or depolarization associated with channel activity could increase endocytic pathways that have been implicated in uptake of aminoglycosides (64). Regardless of the underlying mechanism, our data establish drug hypersensitivity as a useful surrogate for ion channel activity. The simplicity of the assays we have developed to measure drug hypersensitivity (7) makes them particularly appropriate for some applications such as high-throughput screening, where electrophysiological recording of channel activity would not be feasible.

Common Structural Domains Control Both the Functional Activity of PrP^C and Its Conversion to PrP^{Sc}—Although a high resolution structure for PrP^{Sc} has not yet been experimentally determined, a substantial amount of information has accumulated concerning the regions of the PrP molecule that play a role in conversion to the PrP^{Sc} state (see for example Refs. 65, 66, and 67). Importantly, two of these regions (23–31 and 95–125) overlap with those that we have shown here to be critical for the functional activity of PrP^C, as determined by the DBCA and patch clamp measurements. Ligands (GAGs and monoclonal antibodies) that bind to these two regions have been shown to inhibit PrP^{Sc} formation *in vitro* and *in vivo* (16, 68, 69). Strikingly, we have found that some of these same ligands (*e.g.* pentosan polysulfate and mAbs 6D11 and D13) block the ion channel and drug-sensitizing activities of ΔCR PrP (7, 9). In addition, residues 23–33 and 98–110 represent part of the PrP^C-PrP^{Sc} replicative interface, as defined by binding of motif-grafted antibodies (70). Taken together, these data suggest that common structural domains control both the functional activity of PrP^C and its ability to be converted to PrP^{Sc}. Therefore, compounds capable of inhibiting ΔCR PrP toxicity in our cell assays may also be effective in blocking generation of PrP^{Sc} and may, thus, represent therapeutic agents for treatment of prion diseases. Residues 23–27 and 95–110 of PrP^C have also been shown to bind oligomers of the Alzheimer Aβ peptide (71, 72). Thus, the synaptotoxic effect of these oligomers may depend on alterations in the functional activity of PrP^C, and ligands that inhibit PrP^C activity may also block Aβ toxicity.

Acknowledgments—We thank Tim Wilding, Joe Amatrudo, and Jennifer Leubke for advice and technical assistance with patch clamp.

REFERENCES

1. Prusiner, S. B. (1998) *Proc. Natl. Acad. Sci. U.S.A.* **95,** 13363–13383
2. Prusiner, S. B. (ed) (2004) *Prion Biology and Diseases*, 2nd Ed., Cold Spring Harbor Laboratory Press, Cold Spring Harbor, New York
3. Büeler, H., Aguzzi, A., Sailer, A., Greiner, R. A., Autenried, P., Aguet, M., and Weissmann, C. (1993) *Cell* **73,** 1339–1347
4. Brandner, S., Isenmann, S., Raeber, A., Fischer, M., Sailer, A., Kobayashi, Y., Marino, S., Weissmann, C., and Aguzzi, A. (1996) *Nature* **379,** 339–343
5. Mallucci, G., Dickinson, A., Linehan, J., Klöhn, P. C., Brandner, S., and Collinge, J. (2003) *Science* **302,** 871–874
6. Harris, D. A., and True, H. L. (2006) *Neuron* **50,** 353–357
7. Massignan, T., Stewart, R. S., Biasini, E., Solomon, I. H., Bonetto, V., Chiesa, R., and Harris, D. A. (2010) *J. Biol. Chem.* **285,** 7752–7765
8. Massignan, T., Biasini, E., and Harris, D. A. (2011) *Methods* **53,** 214–219
9. Solomon, I. H., Huettner, J. E., and Harris, D. A. (2010) *J. Biol. Chem.* **285,** 26719–26726
10. Li, A., Christensen, H. M., Stewart, L. R., Roth, K. A., Chiesa, R., and Harris, D. A. (2007) *EMBO J.* **26,** 548–558
11. Christensen, H. M., and Harris, D. A. (2009) *J. Neurochem.* **108,** 44–56
12. Bolton, D. C., Seligman, S. J., Bablanian, G., Windsor, D., Scala, L. J., Kim, K. S., Chen, C. M., Kascsak, R. J., and Bendheim, P. E. (1991) *J. Virol.* **65,** 3667–3675
13. Lehmann, S., and Harris, D. A. (1996) *J. Biol. Chem.* **271,** 1633–1637
14. Gorodinsky, A., and Harris, D. A. (1995) *J. Cell Biol.* **129,** 619–627
15. Hobman, T. C., Woodward, L., and Farquhar, M. G. (1995) *Mol. Biol. Cell* **6,** 7–20
16. Pankiewicz, J., Prelli, F., Sy, M. S., Kascsak, R. J., Kascsak, R. B., Spinner, D. S., Carp, R. I., Meeker, H. C., Sadowski, M., and Wisniewski, T. (2006) *Eur. J. Neurosci.* **23,** 2635–2647
17. Korth, C., Stierli, B., Streit, P., Moser, M., Schaller, O., Fischer, R., Schulz-Schaeffer, W., Kretzschmar, H., Raeber, A., Braun, U., Ehrensperger, F., Hornemann, S., Glockshuber, R., Riek, R., Billeter, M., Wüthrich, K., and Oesch, B. (1997) *Nature* **390,** 74–77
18. Huettner, J. E., Lu, A., Qu, Y., Wu, Y., Kim, M., and McDonald, J. W. (2006) *Stem Cells* **24,** 1654–1667
19. Wilding, T. J., Zhou, Y., and Huettner, J. E. (2005) *J. Neurosci.* **25,** 9470–9478
20. Fivaz, M., Vilbois, F., Thurnheer, S., Pasquali, C., Abrami, L., Bickel, P. E., Parton, R. G., and van der Goot, F. G. (2002) *EMBO J.* **21,** 3989–4000
21. Biasini, E., Tapella, L., Restelli, E., Pozzoli, M., Massignan, T., and Chiesa, R. (2010) *Biochem. J.* **430,** 477–486
22. Riek, R., Hornemann, S., Wider, G., Glockshuber, R., and Wüthrich, K. (1997) *FEBS Lett.* **413,** 282–288
23. Knaus, K. J., Morillas, M., Swietnicki, W., Malone, M., Surewicz, W. K., and Yee, V. C. (2001) *Nat. Struct. Biol.* **8,** 770–774
24. Shyng, S. L., Moulder, K. L., Lesko, A., and Harris, D. A. (1995) *J. Biol. Chem.* **270,** 14793–14800
25. Warner, R. G., Hundt, C., Weiss, S., and Turnbull, J. E. (2002) *J. Biol. Chem.* **277,** 18421–18430
26. Wadia, J. S., Schaller, M., Williamson, R. A., and Dowdy, S. F. (2008) *PLoS One* **3,** e3314
27. Sunyach, C., Jen, A., Deng, J., Fitzgerald, K. T., Frobert, Y., Grassi, J., McCaffrey, M. W., and Morris, R. (2003) *EMBO J.* **22,** 3591–3601
28. Hornshaw, M. P., McDermott, J. R., and Candy, J. M. (1995) *Biochem. Biophys. Res. Comm.* **207,** 621–629
29. Pauly, P. C., and Harris, D. A. (1998) *J. Biol. Chem.* **273,** 33107–33110
30. Stahl, N., Borchelt, D. R., Hsiao, K., and Prusiner, S. B. (1987) *Cell* **51,** 229–240
31. Naslavsky, N., Stein, R., Yanai, A., Friedlander, G., and Taraboulos, A.

(1997) *J. Biol. Chem.* **272,** 6324–6331
32. Chesebro, B., Trifilo, M., Race, R., Meade-White, K., Teng, C., LaCasse, R., Raymond, L., Favara, C., Baron, G., Priola, S., Caughey, B., Masliah, E., and Oldstone, M. (2005) *Science* **308,** 1435–1439
33. Jackson, M. R., Nilsson, T., and Peterson, P. A. (1990) *EMBO J.* **9,** 3153–3162
34. Ma, J., Wollmann, R., and Lindquist, S. (2002) *Science* **298,** 1781–1785
35. Drisaldi, B., Stewart, R. S., Adles, C., Stewart, L. R., Quaglio, E., Biasini, E., Fioriti, L., Chiesa, R., and Harris, D. A. (2003) *J. Biol. Chem.* **278,** 21732–21743
36. Baumann, F., Tolnay, M., Brabeck, C., Pahnke, J., Kloz, U., Niemann, H. H., Heikenwalder, M., Rülicke, T., Bürkle, A., and Aguzzi, A. (2007) *EMBO J.* **26,** 538–547
37. Bremer, J., Baumann, F., Tiberi, C., Wessig, C., Fischer, H., Schwarz, P., Steele, A. D., Toyka, K. V., Nave, K. A., Weis, J., and Aguzzi, A. (2010) *Nat. Neurosci.* **13,** 310–318
38. Ivanova, L., Barmada, S., Kummer, T., and Harris, D. A. (2001) *J. Biol. Chem.* **276,** 42409–42421
39. Lorenz, H., Windl, O., and Kretzschmar, H. A. (2002) *J. Biol. Chem.* **277,** 8508–8516
40. Peretz, D., Williamson, R. A., Matsunaga, Y., Serban, H., Pinilla, C., Bastidas, R. B., Rozenshteyn, R., James, T. L., Houghten, R. A., Cohen, F. E., Prusiner, S. B., and Burton, D. R. (1997) *J. Mol. Biol.* **273,** 614–622
41. Pan, K. M., Baldwin, M., Nguyen, J., Gasset, M., Serban, A., Groth, D., Mehlhorn, I., Huang, Z., Fletterick, R. J., Cohen, F. E., and Prusiner, S. B. (1993) *Proc. Natl. Acad. Sci. U.S.A.* **90,** 10962–10966
42. Pasupuleti, M., Roupe, M., Rydengård, V., Surewicz, K., Surewicz, W. K., Chalupka, A., Malmsten, M., Sörensen, O. E., and Schmidtchen, A. (2009) *PLoS One* **4,** e7358
43. Hooper, N. M., Taylor, D. R., and Watt, N. T. (2008) *Biochem. Soc. Trans.* **36,** 1272–1276
44. Baumann, F., Pahnke, J., Radovanovic, I., Rülicke, T., Bremer, J., Tolnay, M., and Aguzzi, A. (2009) *PLoS One* **4,** e6707
45. Khosravani, H., Zhang, Y., Tsutsui, S., Hameed, S., Altier, C., Hamid, J., Chen, L., Villemaire, M., Ali, Z., Jirik, F. R., and Zamponi, G. W. (2008) *J. Cell Biol.* **181,** 551–565
46. Collinge, J., Whittington, M. A., Sidle, K. C., Smith, C. J., Palmer, M. S., Clarke, A. R., and Jefferys, J. G. (1994) *Nature* **370,** 295–297
47. Maglio, L. E., Perez, M. F., Martins, V. R., Brentani, R. R., and Ramirez, O. A. (2004) *Brain Res. Mol. Brain Res.* **131,** 58–64
48. Herms, J. W., Tings, T., Dunker, S., and Kretzschmar, H. A. (2001) *Neurobiol. Dis.* **8,** 324–330
49. Fuhrmann, M., Bittner, T., Mitteregger, G., Haider, N., Moosmang, S., Kretzschmar, H., and Herms, J. (2006) *J. Neurochem.* **98,** 1876–1885
50. Shmerling, D., Hegyi, I., Fischer, M., Blättler, T., Brandner, S., Götz, J., Rülicke, T., Flechsig, E., Cozzio, A., von Mering, C., Hangartner, C., Aguzzi, A., and Weissmann, C. (1998) *Cell* **93,** 203–214
51. Zanata, S. M., Lopes, M. H., Mercadante, A. F., Hajj, G. N., Chiarini, L. B., Nomizo, R., Freitas, A. R., Cabral, A. L., Lee, K. S., Juliano, M. A., de Oliveira, E., Jachieri, S. G., Burlingame, A., Huang, L., Linden, R., Brentani, R. R., and Martins, V. R. (2002) *EMBO J.* **21,** 3307–3316
52. Hajj, G. N., Lopes, M. H., Mercadante, A. F., Veiga, S. S., da Silveira, R. B., Santos, T. G., Ribeiro, K. C., Juliano, M. A., Jacchieri, S. G., Zanata, S. M., and Martins, V. R. (2007) *J. Cell Sci.* **120,** 1915–1926
53. Hay, B., Barry, R. A., Lieberburg, I., Prusiner, S. B., and Lingappa, V. R. (1987) *Mol. Cell. Biol.* **7,** 914–920
54. Yost, C. S., Lopez, C. D., Prusiner, S. B., Myers, R. M., and Lingappa, V. R. (1990) *Nature* **343,** 669–672
55. Mead, S. (2006) *Eur. J. Hum. Genet.* **14,** 273–281
56. Riek, R., Wider, G., Billeter, M., Hornemann, S., Glockshuber, R., and Wüthrich, K. (1998) *Proc. Natl. Acad. Sci. U.S.A.* **95,** 11667–11672
57. Apetri, A. C., Surewicz, K., and Surewicz, W. K. (2004) *J. Biol. Chem.* **279,** 18008–18014
58. Zhang, Y., Swietnicki, W., Zagorski, M. G., Surewicz, W. K., and Sönnichsen, F. D. (2000) *J. Biol. Chem.* **275,** 33650–33654
59. Telling, G. C., Haga, T., Torchia, M., Tremblay, P., DeArmond, S. J., and Prusiner, S. B. (1996) *Genes Dev.* **10,** 1736–1750
60. Rodriguez, M. M., Peoc'h, K., Haïk, S., Bouchet, C., Vernengo, L., Mañana, G., Salamano, R., Carrasco, L., Lenne, M., Beaudry, P., Launay, J. M., and Laplanche, J. L. (2005) *Neurology* **64,** 1455–1457
61. Marcotti, W., van Netten, S. M., and Kros, C. J. (2005) *J. Physiol.* **567,** 505–521
62. Myrdal, S. E., Johnson, K. C., and Steyger, P. S. (2005) *Hear. Res.* **204,** 156–169
63. Myrdal, S. E., and Steyger, P. S. (2005) *Hear. Res.* **204,** 170–182
64. Sandoval, R. M., Dunn, K. W., and Molitoris, B. A. (2000) *Am. J. Physiol. Renal Physiol.* **279,** F884–F890
65. Kourie, J. I., Kenna, B. L., Tew, D., Jobling, M. F., Curtain, C. C., Masters, C. L., Barnham, K. J., and Cappai, R. (2003) *J. Membr. Biol.* **193,** 35–45
66. Norstrom, E. M., and Mastrianni, J. A. (2005) *J. Biol. Chem.* **280,** 27236–27243
67. Kourie, J. I. (2002) *Eur. Biophys. J.* **31,** 409–416
68. Doh-ura, K., Ishikawa, K., Murakami-Kubo, I., Sasaki, K., Mohri, S., Race, R., and Iwaki, T. (2004) *J. Virol.* **78,** 4999–5006
69. White, A. R., Enever, P., Tayebi, M., Mushens, R., Linehan, J., Brandner, S., Anstee, D., Collinge, J., and Hawke, S. (2003) *Nature* **422,** 80–83
70. Solforosi, L., Bellon, A., Schaller, M., Cruite, J. T., Abalos, G. C., and Williamson, R. A. (2007) *J. Biol. Chem.* **282,** 7465–7471
71. Chen, S., Yadav, S. P., and Surewicz, W. K. (2010) *J. Biol. Chem.* **285,** 26377–26383
72. Laurén, J., Gimbel, D. A., Nygaard, H. B., Gilbert, J. W., and Strittmatter, S. M. (2009) *Nature* **457,** 1128–1132